Adıyaman University Journal of Science
https://dergipark.org.tr/en/pub/adyujsci
DergiPark AKADEMİK
ISSN 2147-1630
e-ISSN 2146-586X

In-depth Profiling of *N*-glycans Isolated from Ostrich Egg White and Yolk Glycoproteomes by HPLC-HILIC-FLD-MS/MS

Hacı Mehmet KAYILI[1,*]

[1]*Karabük University, Department of Biomedical Engineering, Karabük, Turkey*
h.mehmetkayili@karabuk.edu.tr, ORCID: 0000-0002-6740-0645

Received: 07.05.2020 **Accepted:** 31.05.2020 **Published:** 30.06.2021

Abstract

Protein glycosylation is an essential post-translational modification and modulates critical cellular events. It is known that *N*-glycosylated proteins from egg white and yolk are played crucial roles in various cellular pathways. Characterization of *N*-glycan structures of glycoproteomes is required to understand these functions. Therefore, this study is aimed to characterize the *N*-glycan profiles of ostrich egg white and yolk glycoproteomes. In the study, *N*-glycans were released from ostrich egg white and yolk glycoproteomes by an enzymatical process and labeled with a procainamide tag. Samples were analyzed by HPLC-HILIC-FLD-MS/MS (high-performance hydrophilic interaction liquid chromatography with fluorescence and tandem mass spectrometric detection). The number of detected *N*-glycans obtained from ostrich egg white and yolk glycoproteomes was found to be 39 and 36, respectively. It was determined that *N*-glycans of ostrich egg white glycoproteome were highly galactosylated (96.64%). In addition, bisecting *N*-glycans were abundant in ostrich egg white glycoproteome (91.72%) compared to ostrich egg yolk glycoproteome (6.74%). The abundance of high-mannose *N*-glycans was dramatically higher in the ostrich egg yolk glycoproteome (55.84%) than the ostrich egg yolk glycoproteome (2.67%). The fucosylation ratio of *N*-glycans belonging to ostrich egg white and yolk glycoproteomes was detected to be 4.52% and 0.95%, respectively. The obtained data

* Corresponding Author DOI: 10.37094/adyujsci.934336

showed that *N*-glycan profiles of ostrich egg white and yolk glycoproteomes differed significantly.

Keywords: Glycosylation; Glycomics; Ostrich egg white; Ostrich egg yolk; HPLC; Mass spectrometry.

Devekuşu Yumurta Akı ve Sarısı Glikoproteomlarından İzole Edilmiş *N*-glikanların HPLC-HILIC-FLD-MS/MS ile Derinlemesine Profillenmesi

Öz

Protein glikozilasyonu önemli bir post-translasyonel modifikasyondur ve kritik hücresel olayları kontrol eder. Yumurta akı ve sarısından elde edilen *N*-glikozile proteinlerin çeşitli hücresel yolaklarda önemli roller oynadığı bilinmektedir. Bu fonksiyonları anlamak için glikoproteomlara ait *N*-glikan yapılarının karakterizasyonu gereklidir. Bu nedenle, bu çalışma devekuşu yumurtası akı ve yumurta sarısı glikoproteomlarının *N*-glikan profillerini karakterize etmeyi amaçlamaktadır. Çalışmada, devekuşu yumurta akı ve sarısı glikoproteomlarından *N*-glikanlar enzimatik bir süreçle salındı ve bir prokainamid etiketi ile etiketlendi. Örnekler, HPLC-HILIC-FLD-MS/MS (yüksek performanslı hidrofilik etkileşim sıvı kromatografisi ile floresans ve ikili kütle spektrometrik dedeksiyon) ile analiz edildi. Devekuşu yumurta akı ve sarısı glikoproteomlarından tespit edilen *N*-glikan sayıları sırasıyla 39 ve 36 olarak bulundu. Devekuşu yumurtası akı glikoproteomunun *N*-glikanlarının yüksek oranda galaktozile olduğu (%96,64) belirlendi. Ek olarak, bisekte *N*-glikanların devekuşu yumurtası akı glikoproteomunda (%91.72) devekuşu yumurta sarısı glikoproteomuna (%6.74) kıyasla bol miktarda bulunmuştur. Devekuşu yumurta sarısı glikoproteomunda yüksek mannozlu *N*-glikanların bolluğu (%55.84) devekuşu yumurta sarısı glikoproteomundan (%2.67) önemli ölçüde daha yüksek olduğu belirlendi. Devekuşu yumurtası akı ve sarısı glikoproteomlarına ait *N*-glikanların fukozlanma oranı sırasıyla %4.52 ve %0.95 olarak tespit edilmiştir. Elde edilen veriler, devekuşu yumurtası akı ve sarısı glikoproteomlarının *N*-glikan profillerinin önemli ölçüde farklılık gösterdiğini göstermiştir.

Anahtar Kelimeler: Glikozilasyon; Glikomik; Devekuşu yumurtası akı; Devekuşu yumurta sarısı; HPLC; Kütle spektrometresi.

1. Introduction

Proteins can be modified covalently after the translation step of the protein synthesis process [1]. These modifications, named post-translational modifications, are prevalent in eukaryote proteomes [2]. Glycosylation is one of the most observed types among post-translational modifications. Complex oligosaccharides called glycans attach to proteins by several

enzymatical pathways. By this attachment, the function of the glycosylated proteins is dramatically changed depending on the structures of the glycans [3]. In addition, glycosylated proteins modulate critical biological events in organisms [4]. It is known that glycosylation process changes in various acute diseases [5].

N-glycosylated proteins from egg white and yolk are played essential roles in cellular events. For example, it has been reported that ovomicin glycoprotein in egg white has anti-adhesive, anticancer, and anti-microbial properties against infectious diseases [6]. Derived glycopeptides from ovumicin bind to E-coli, thereby protecting against E-coli infection [7]. Besides, they provide to determine bacteria in foods [8]. In addition to ovomicin, many other glycoproteins containing ovalbumin, ovotransferrin, ovomucoid, ovoglycoprotein are found in egg white. They have unique biological activities such as antihypertensive, antibacterial, anticancer, etc. It has been suggested that glycans inhibit microorganisms by sticking to intestinal cells [9]. Therefore, in-depth *N*-glycan analysis of egg white and yolk is required to detect potential bioactive elements and determine the functions of these glycoproteins.

Glycomics is a multidisciplinary field focused on characterizing glycan structures to determine their roles in cellular events [10]. Mass spectrometry-based glycomics is the most commonly applied strategy for analyzing glycans derived from different biological samples [11]. Tandem mass spectrometry is allowed to identify *N*-glycan structures; however, ionization efficiencies of glycans are very low in the mass spectrometric analysis [12-14]. On the other hand, HPLC-HILIC-FLD is a golden standard method for quantitative glycomics. *N*-glycans are labeled with fluorophore tags from their reducing ends in this approach. Recently, a fluorophore tag named procainamide which increases both MS and FLD signals has been introduced to analyze glycans [15, 16]. When this approach is combined with tandem mass spectrometry, both qualitative and quantitative information is obtained. In addition, some essential *N*-glycan types, including bisecting and core fucosylated glycans, can be detected using tandem mass spectrometry, thereby profiling almost all detected *N*-glycans by this approach [17, 18].

Here, a study was undertaken for in-depth profiling of ostrich egg white and yolk *N*-glycans using a glycomics approach. Glycans were first released from glycoproteins extracted from ostrich egg white and yolk proteomes and labeled with procainamide tag. Analysis was achieved using HPLC-HILIC-FLD-MS/MS. Structural analysis of *N*-glycans was performed by tandem mass spectrometry, whereas quantitative data for each detected *N*-glycans were obtained from FLD detection. Thus, *N*-glycans belonging to ostrich egg white and yolk glycoproteins were identified and quantified.

2. Materials and Methods

2.1. Materials

Unless otherwise stated, all chemicals used in the study were purchased from Sigma Aldrich (St Louis, MO, USA). Procainamide HCl was bought from Abcam (Cambridge, UK). PNGase F enzyme was obtained from Promega (Madison, WI, USA). Ostrich eggs were obtained from a local farm in Turkey.

2.2. Glycan release

Approximately 2 mg of lyophilized ostrich egg white and yolk were dissolved with 100 µL of 2% SDS (w/v) and incubated at 60 ^{o}C for 10 min by vigorously shaking. Then, 50 µL of 4 % Igepal-CA630 (v/v) and 50 µL of 5X PBS were inserted to the samples. Finally, 1 U of PNGase F enzyme (1 U μL^{-1}) was inserted, and the samples were incubated at 37 ^{o}C overnight.

2.3. Procainamide labeling

The samples were mixed with 100 µL of a labeling solution including 50 µL of procainamide hydrochloride (110 mg mL^{-1} in DMSO/AA, 7/3, v/v) and 50 µL of sodiumcyano bor hydride (60 mg mL^{-1} in DMSO/AA, 7/3, v/v). Subsequently, the samples were incubated at 65 ^{o}C for 2 h.

2.4. Purification of procainamide labeling glycans

The procainamide labeled *N*-glycans were purified using microcrystalline cellulose. First, 200 µL of microcrystalline cellulose (0.1 mg mL^{-1} in dH_2O) was transferred to microtubes and washed with 1 mL of dH_2O and 85% ACN two times, respectively. Then, 150 µL of labeled *N*-glycans and 850 µL of ACN were inserted into microcrystalline cellulose-containing microtubes. The samples were incubated for 20 min at room temperature by vigorously shaking. Then, the mixtures were transferred to 1 mL capacity sep-pack cartridges. To remove impurities and excess dye, microcrystalline cellulose was washed by 1 ml of 85% ACN including 1% TFA and 1 mL of 85% ACN three times, respectively. Finally, the elution of the procainamide labeled *N*-glycans were achieved by 750 µL of dH_2O. The elutions were then dried using a speed vacuum concentrator. The samples were dissolved with 100 µL of 75% ACN prior to their analysis with HPLC-HILIC-FLD-MS/MS.

2.5. HPLC-HILIC-FLD-MS/MS analysis

HPLC-HILIC-FLD-MS/MS analysis of procainamide labeled *N*-glycans of ostrich egg white and yolk was carried out by a Bruker TIMS-TOF mass spectrometry (Bruker Daltonik GmbH, Bremen, Germany) combined with an Agilent 1200 series HPLC system containing 1260 series FLD detector. A tee connection was used to separate pump flow into the two equal volumes for MS and FLD detections. The mobile phases (A: 50 mM ammonium formate pH: 4.4; B: 100% ACN) were used for analytical separations of procainamide labeled *N*-glycans. The gradient program was applied by decreasing the mobile phase B from 75% to 53% within 60 min. Waters Glycan BEH Amide 2,5 µm (2.1 mm ID x 15 cm L) HILIC column was employed in the analytical separations of the *N*-glycans. The excitation and emission wavelength of the FLD detector were adjusted to 310 nm and 370 nm, respectively. The flow rate was set to 0.35 mL min^{-1}. The injection volume was 40 µL.

For MS parameters, the capillary voltage was adjusted to 4.5 kV. Source temperature was 250 ^{o}C. Nebulizer and drying gases were set to 1.7 bar and 6 L min^{-1}, respectively. MS acquisition was achieved from 400 to 2500 m/z at a frequency of 1 Hz. The three most abundant precursors were selected at a spectra rate of 0.5 Hz to 2 Hz or MS/MS experiments.

2.6. Data analysis

The MS/MS spectra were first imported to Protein Scape Software (Bruker Daltonik GmbH, Bremen, Germany). GlycoQuest algorithm (search engine) was used to identify procainamide labeled *N*-glycans. Carbbank was selected as a database. MS and MS/MS tolerances were adjusted to 20 ppm and 0.05 Da. The obtained MS/MS spectra were also manually checked to determine *N*-glycan structures as well as identifying *N*-glycan types. The relative abundances of the detected FLD peaks were calculated by performing a total area normalization approach. To achieve this, the relative abundance of a glycan peak was found as follows:

Relative Abundance% = area of an *N*-glycan peak / the summed areas of *N*-glycan peaks *100

Statistical tests were performed using Graphpad Prism 9 software. Multiple t-tests was applied to compare *N*-glycan trait abundances between the ostrich egg white and yolk glycoproteomes. A probability value ($p < 0.01$) was considered statistically significant.

3. Results and Discussion

3.1. *N*-glycan profiling of ostrich egg white

N-glycans were released from ostrich egg white and labeled with procainamide. After purifications of procainamide labeled *N*-glycans, analyses were achieved by HPLC-HILIC-FLD-

MS/MS system. MS detection was used for the identification of procainamide labeled *N*-glycan structures, whereas FLD detection was performed for the relative quantification of procainamide labeled *N*-glycans. The FLD and BPC (base peak chromatogram) chromatograms of ostrich egg yolk were shown in Fig. 1. Thirty-one peaks were detected in the FLD and BPC chromatograms. When the MS/MS data searched against a Carbbank database using the glycoQuest algorithm, thirty-nine different *N*-glycan structures were determined under these peaks. High-mannose, complex, hybrid, and bisected *N*-glycan types were detected. A list obtained from Proteinscape Software were displayed in Table 1.

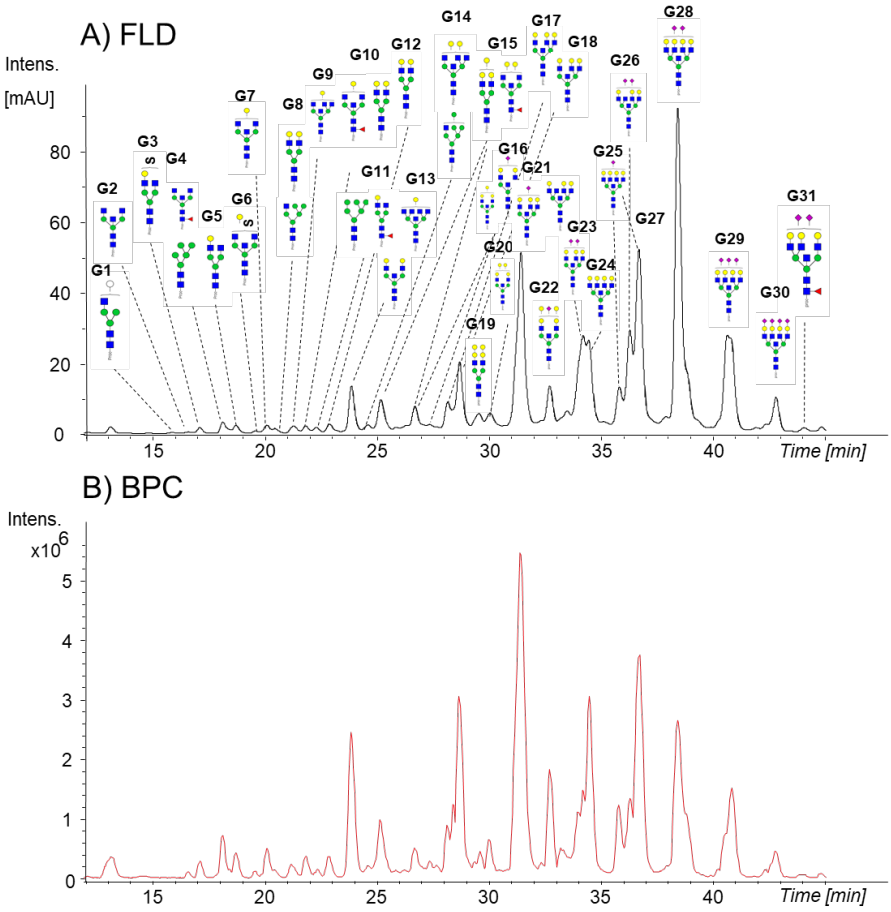

Figure 1: Fluorescence (A) and base peak chromatograms (B) of procainamide labeled *N*-glycans released from glycoproteins extracted from ostrich egg white

As shown in Fig. 1, di-, tri-, and tetra-antennary glycan types *N*-glycan structures were determined. On the other hand, most of the detected *N*-glycans did not include sialic acid residues; however, sialic acid-containing *N*-glycans were the most abundant types in the related chromatogram. Sulfated *N*-glycan types with minor amounts were also detected by the analysis of the samples using HPLC-HILIC-FLD-MS/MS. It was determined that all the fucosylated glycans were core-fucosylated by following the MS/MS fragments highlighted previously in the

literature [18]. Besides, bisected *N*-glycans were confirmed by checking the specific fragments described in the literature for bisecting *N*-glycans [17].

Table 1: The list of procainamide labeled *N*-glycans belonging to ostrich egg white glycoproteome. nd: non-detected by glycoQuest and manually identified

Peak	*N*-glycan Composition	m/z meas.	z	m/z calc.	Δm/z Da	Δm/z ppm	Rt min	Scor.	Frg. Cv. %
G1	Hex4HexNAc3	748.3294	2	748.3240	0.0053	7.10	16.05	75.5	58
G2	Hex3HexNAc5	870.3830	2	870.3770	0.0060	6.88	16.63	119.7	172
G3	Hex4HexNAc4S1	889.8476	2	889.8421	0.0054	6.09	17.06	79.9	73
G4	Hex5HexNAc2	727.8140	2	727.8108	0.0033	4.47	18.06	96.9	105
G4	Hex3HexNAc5dHex1	943.4092	2	943.4060	0.0032	3.41	18.31	90.4	90
G5	Hex4HexNAc4	849.8676	2	849.8637	0.0038	4.52	18.65	105.0	118
G6	Hex4HexNAc5S1	661.2605	3	661.2570	0.0036	5.40	19.57	81.6	70
G7	Hex4HexNAc5	951.4090	2	951.4034	0.0056	5.89	20.14	128.4	175
G8	Hex5HexNAc3	829.3548	2	829.3505	0.0043	5.22	20.39	92.5	98
G8	Hex5HexNAc4	620.9326	3	620.9292	0.0034	5.49	20.43	50.6	32
G8	Hex4HexNAc5	951.4070	2	951.4034	0.0036	3.79	20.65	94.0	113
G9	Hex4HexNAc6	1052.9466	2	1052.9431	0.0035	3.32	21.41	118.3	185
G9	Hex5HexNAc4	930.8946	2	930.8901	0.0044	4.76	21.59	84.9	80
G9	Hex4HexNAc5dHex1	1024.4372	2	1024.4324	0.0048	4.67	21.64	52.0	30
G10	Hex5HexNAc4	930.8950	2	930.8901	0.0048	5.18	21.73	113.3	148
G10	Hex4HexNAc5dHex1	1024.4378	2	1024.4324	0.0054	5.30	21.74	84.7	84
G11	Hex4HexNAc4dHex1	922.8974	2	922.8927	0.0047	5.10	22.23	68.8	79
G11	Hex6HexNAc2	808.8415	2	808.8372	0.0043	5.31	22.32	101.5	135
G13	Hex5HexNAc5	688.6270	3	688.6223	0.0047	6.87	23.72	146.6	230
G13	Hex4HexNAc7	769.9960	3	769.9909	0.0050	6.50	24.28	82.9	78
G14	Hex5HexNAc3NeuAc1	650.2719	3	650.2679	0.0041	6.24	24.34	60.4	43
G14	Hex6HexNAc3	910.3818	2	910.3769	0.0049	5.42	24.57	101.9	116
G14	Hex5HexNAc6	756.3206	3	756.3154	0.0051	6.79	24.86	125.7	186
G15	Hex5HexNAc6	1133.9764	2	1133.9695	0.0069	6.10	24.88	122.2	183
G15	Hex6HexNAc4	1011.9211	2	1011.9165	0.0045	4.47	24.97	107.0	127
G15	Hex5HexNAc5dHex1	737.3129	3	737.3083	0.0046	6.22	25.39	93.2	99
G16	Hex5HexNAc5NeuAc1	785.6599	3	785.6541	0.0058	7.42	26.55	88.2	92
G16	Hex6HexNAc5	742.6459	3	742.6399	0.0060	8.05	26.64	115.0	169
G17	Hex6HexNAc6	810.3392	3	810.3330	0.0062	7.65	28.13	151.5	255
G18	Hex6HexNAc6	810.3393	3	810.3330	0.0062	7.68	28.59	175.8	362
G19	Hex7HexNAc4	728.9705	3	728.9644	0.0061	8.31	29.27	110.5	158
G20	Hex6HexNAc5NeuAc1	1259.0120	2	1259.0039	0.0081	6.42	29.85	54.9	42
G20	Hex7HexNAc5	796.6634	3	796.6575	0.0059	7.38	29.88	123.2	196
G20	Hex5HexNAc5NeuAc2	882.6925	3	882.6859	0.0066	7.47	30.07	65.2	68
G21	Hex6HexNAc6NeuAc1	907.3726	3	907.3648	0.0078	8.60	31.00	nd	nd
G21	Hex6HexNAc7	878.0341	3	878.0262	0.0079	8.98	31.68	140.7	216
G22	Hex7HexNAc5NeuAc1	893.6965	3	893.6893	0.0072	8.06	32.50	nd	nd
G23	Hex6HexNAc6NeuAc2	1004.4034	3	1004.3967	0.0067	6.70	33.71	59.0	62
G24	Hex7HexNAc7	932.0509	3	932.0438	0.0072	7.69	33.93	103.4	190
G25	Hex7HexNAc7NeuAc1	1029.0827	3	1029.0756	0.0071	6.90	35.80	nd	nd

G26	Hex6HexNAc7NeuAc2	1072.0964	3	1072.0898	0.0066	6.16	36.20	nd	nd
G27	Hex7HexNAc7NeuAc1	1029.0819	3	1029.0756	0.0063	6.12	36.70	nd	nd
G28	Hex7HexNAc7NeuAc2	1126.1152	3	1126.1074	0.0078	6.93	38.30	nd	nd
G29	Hex7HexNAc7NeuAc3	1223.1470	3	1223.1392	0.0078	6.38	40.50	nd	nd
G30	Hex7HexNAc7NeuAc4	1320.1823	3	1320.1710	0.0113	8.56	42.70	nd	nd
G31	Hex6HexNAc6NeuAc2dHex1	1579.6002	2	1579.6246	-0.0244	-15.4	44.00	nd	nd

Relative abundances of the detected *N*-glycans were calculated by applying the total area normalization approach. The relative abundances of the *N*-glycan peaks for ostrich egg white glycoproteome were shown in Fig. 2. The analysis was achieved with three experimental replicates. The *N*-glycan peak G21 (Hex6HexNAc6NeuAc1, Hex7HexNAc7NeuAc2) was found to be most abundant among *N*-glycan peaks (19.23%). The second most intense *N*-glycan peak was G28 (Hex7HexNAc7NeuAc2, 17.74%). *N*-glycan traits were derived depending on glycan types of the detected *N*-glycans. It was seen that tri- and tetra-antennary type *N*-glycans were the most abundant types compared to mono- and di-antennary *N*-glycan types. The fucosylation ratio was found to be 4.52%, whereas relative abundances of bisected *N*-glycans was 91.72% for ostrich egg white glycoproteome. In addition, the relative abundance of sialylation was found to be 61.70%. High-mannose type was covered to 2.66% within the detected *N*-glycan types of ostrich egg white.

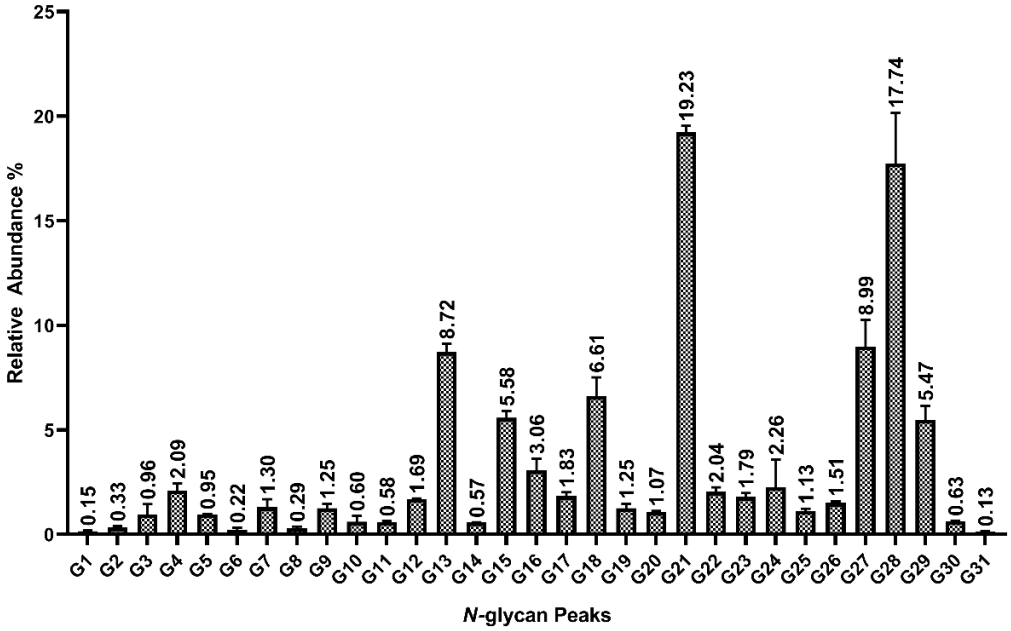

Figure 2: Relative abundances of *N*-glycan Peaks belonging to ostrich egg white glycoproteome

3.2. *N*-glycan profiling of ostrich egg yolk

N-glycans were released from the ostrich egg yolk glycoproteome and labeled with a procainamide tag. The labeled *N*-glycans were then analyzed by HPLC-HILIC-FLD-MS/MS system. The MS and FLD chromatograms of *N*-glycans belonging to ostrich egg yolk glycoproteome were shown in Fig. 3.

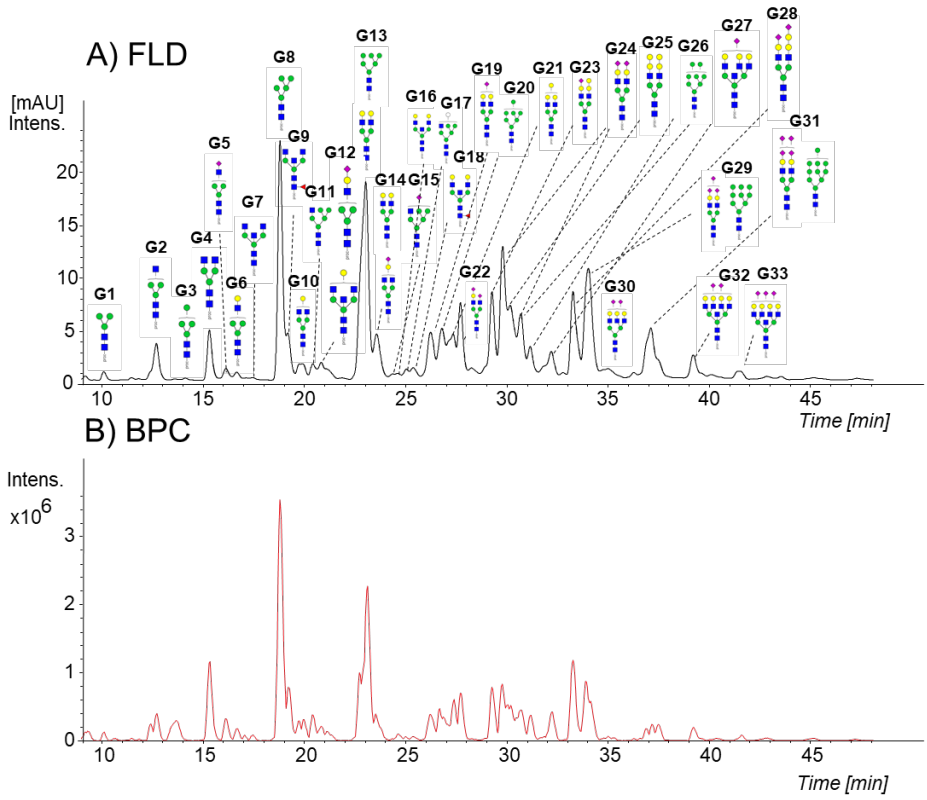

Figure 3: Fluorescence (A) and base peak chromatograms (B) of procainamide labeled *N*-glycans released from glycoproteins extracted from ostrich egg yolk

Thirty-six different *N*-glycan structures were determined by the analysis of obtained MS/MS data, which were detected under 33 *N*-glycan peaks in the FLD chromatogram. Similar to ostrich egg white glycoproteome, high-mannose, complex, hybrid, and bisected *N*-glycan types were determined in the analysis. The list for the detected *N*-glycans from ostrich egg yolk glycoproteome was displayed in Table 2.

Table 2: The list of procainamide labeled *N*-glycans belonging to ostrich egg yolk glycoproteome. nd: non-detected by glycoQuest and manually identified

Peak	*N*-glycan Composition	m/z meas.	z	m/z calc.	Δm/z Da	Δm/z ppm	Rt min	Scor.	Frg. Cv. %
G1	Hex3HexNAc2	565.7571	2	565.7579	-0.0009	-1.50	10.22	82.2	77
G2	Hex3HexNAc3	667.2967	2	667.2976	-0.0009	-1.33	12.70	89.3	89
G3	Hex4HexNAc2	646.7828	2	646.7844	-0.0015	-2.38	14.20	76.8	69
G4	Hex3HexNAc4	768.8367	2	768.8373	-0.0006	-0.78	15.24	95.5	104

G5	Hex3HexNAc3NeuAc1	812.8444	2	812.8453	-0.0009	-1.11	16.10	nd	nd
G6	Hex4HexNAc3	748.3239	2	748.3240	-0.0002	-0.23	16.70	89.2	89
G7	Hex3HexNAc5	870.3758	2	870.3770	-0.0012	-1.40	17.27	84.0	86
G8	Hex5HexNAc2	727.8100	2	727.8108	-0.0008	-1.04	18.81	87.0	83
G9	Hex3HexNAc5dHex1	943.4038	2	943.4060	-0.0022	-2.31	19.08	74.2	77
G10	Hex4HexNAc4	849.8626	2	849.8637	-0.0012	-1.38	19.16	101.0	113
G11	Hex5HexNAc3	829.3497	2	829.3505	-0.0008	-0.95	20.33	103.6	117
G12	Hex4HexNAc3NeuAc1	893.8706	2	893.8717	-0.0012	-1.31	20.96	71.5	57
G12	Hex4HexNAc5	951.4018	2	951.4034	-0.0016	-1.69	20.97	93.0	108
G13	Hex5HexNAc4	930.8894	2	930.8901	-0.0008	-0.84	22.70	108.7	135
G13	Hex4HexNAc4NeuAc1	995.4110	2	995.4114	-0.0004	-0.40	22.84	85.7	80
G13	Hex6HexNAc2	808.8372	2	808.8372	0.0000	0.04	22.99	116.6	148
G14	Hex5HexNAc4	930.8890	2	930.8901	-0.0011	-1.21	23.43	100.9	116
G14	Hex4HexNAc4NeuAc1	995.4099	2	995.4114	-0.0015	-1.50	23.44	80.2	76
G15	Hex5HexNAc3NeuAc1	974.8956	2	974.8982	-0.0025	-2.58	24.41	70.1	55
G16	Hex5HexNAc5	1032.4263	2	1032.4298	-0.0035	-3.41	24.77	96.8	107
G17	Hex6HexNAc3	910.3744	2	910.3769	-0.0024	-2.67	24.91	89.0	90
G18	Hex5HexNAc5dHex1	553.2357	4	553.2330	0.0026	4.76	25.43	51.1	39
G19	Hex5HexNAc4NeuAc1	1076.4359	2	1076.4378	-0.0019	-1.78	26.12	84.4	79
G20	Hex7HexNAc2	889.8618	2	889.8636	-0.0018	-2.02	26.57	115.0	141
G21	Hex6HexNAc4	1011.9144	2	1011.9165	-0.0022	-2.13	26.84	97.0	107
G22	Hex4HexNAc4NeuAc2	760.9747	3	760.9752	-0.0005	-0.70	27.73	97.3	101
G23	Hex6HexNAc4NeuAc1	771.9780	3	771.9786	-0.0006	-0.72	29.23	96.1	97
G24	Hex5HexNAc4NeuAc2	814.9912	3	814.9928	-0.0016	-1.97	29.71	96.8	98
G25	Hex7HexNAc4	728.9635	3	728.9644	-0.0009	-1.18	30.22	112.7	134
G26	Hex8HexNAc2	970.8880	2	970.8900	-0.0020	-2.10	30.35	120.1	155
G27	Hex6HexNAc6NeuAc1	907.3632	3	907.3648	-0.0016	-1.76	nd	nd	nd
G28	Hex6HexNAc4NeuAc2	869.0094	3	869.0104	-0.0010	-1.14	33.17	77.9	68
G29	Hex5HexNAc4NeuAc3	912.0226	3	912.0246	-0.0020	-2.21	33.46	72.8	62
G29	Hex9HexNAc2	1051.9136	2	1051.9164	-0.0028	-2.70	33.56	74.3	81
G30	Hex6HexNAc5NeuAc2	936.7022	3	936.7035	-0.0013	-1.38	34.84	74.1	64
G31	Hex10HexNAc2	1132.9415	2	1132.9428	-0.0013	-1.18	36.74	130.5	190
G31	Hex5HexNAc4NeuAc4	1009.3899	3	1009.3926	-0.0027	-2.68	37.10	77.9	69
G32	Hex7HexNAc7NeuAc2	844.8318	4	844.8324	-0.0006	-0.71	39.10	nd	nd
G33	Hex7HexNAc7NeuAc3	917.6066	4	917.6062	0.0004	0.44	41.50	nd	nd

The relative abundances of the *N*-glycan peaks for ostrich egg white glycoproteome were shown in Fig. 2. The *N*-glycan peak G13 (Hex5HexNAc4, Hex4HexNAc4NeuAc1, and Hex6HexNAc2) was found to be most abundant among *N*-glycan peaks (21.23%). The second most intense *N*-glycan peak was found to be G8 (Hex5HexNAc2, 15.42%). *N*-glycan traits were derived depending on glycan types of the detected *N*-glycans. It was noticed that the fucosylation ratio was found to be 0.95%. At the same time, relative abundances of bisected *N*-glycans was 6.74% for ostrich egg yolk glycoproteome. In addition, the relative abundance of sialylation was found to be 46.40%. High-mannose type was covered to 55.84% within the detected *N*-glycan types for ostrich egg yolk.

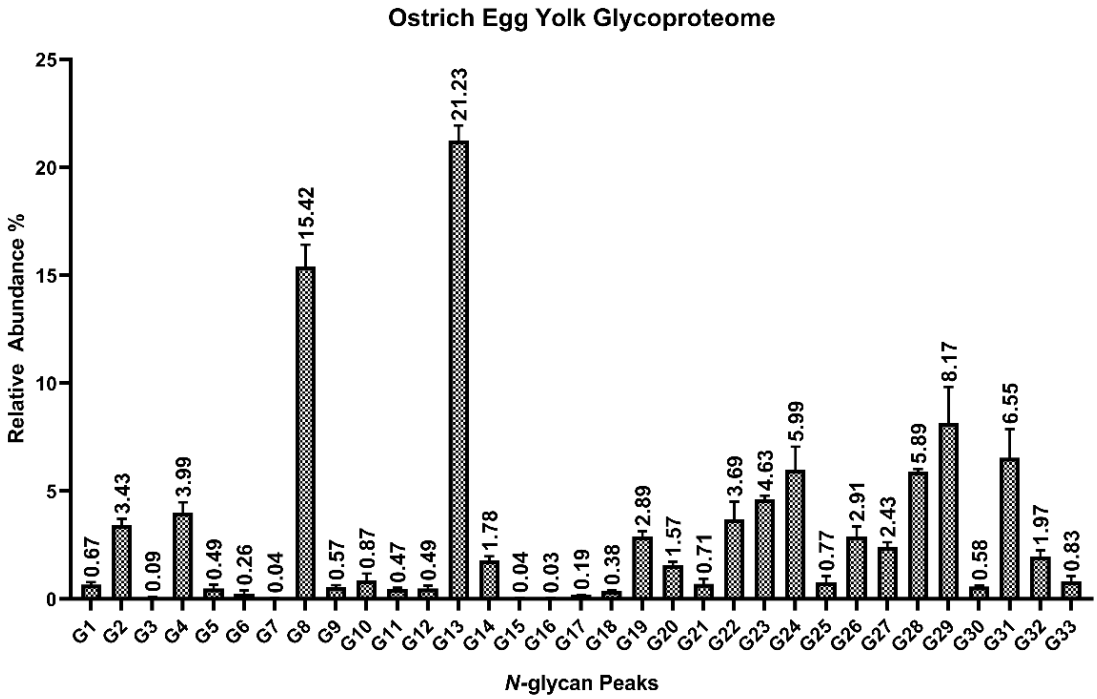

Figure 4: Relative abundances of *N*-glycan Peaks belonging to ostrich egg yolk glycoproteome

3.3. Comparison of *N*-glycan types and traits between ostrich egg white and yolk glycoproteome

The type of the detected *N*-glycans was compared in the study for ostrich egg white and yolk glycoproteomes. The results showed that the 18 *N*-glycan structures were identified in both species. Twenty-one *N*-glycan structures were only found in the ostrich egg white glycoproteome, whereas 19 *N*-glycan structures were detected in the ostrich egg yolk glycoproteome. Bisected *N*-glycan types were more abundant in ostrich egg white glycoproteome than ostrich egg yolk. However, the number of high-mannose *N*-glycan types detected by the analysis of ostrich egg yolk glycoproteome was higher compared with ostrich egg white glycoproteome.

The relative abundances of *N*-glycan traits were derived from *N*-glycans detected from the analysis using HPLC-HILIC-FLD-MS/MS for both ostrich egg white and yolk glycoproteomes. The comparisons of derived *N*-glycan traits were shown in Fig. 5. The fucosylation ratio was found to be low for both glycoproteomes. The relative abundance of bisecting *N*-glycans was dramatically abundant in ostrich egg white glycoproteome (91.72%). In contrast, high-mannose *N*-glycans were covered abundantly in ostrich egg yolk glycoproteome (55.84%). The *N*-glycans of ostrich egg white glycoproteome was highly galactosylated (96.64%), while this was 72.38%

for the *N*-glycans of ostrich egg yolk glycoproteome. Sialylation of ostrich egg white glycoproteome was higher than that of ostrich egg yolk glycoproteome.

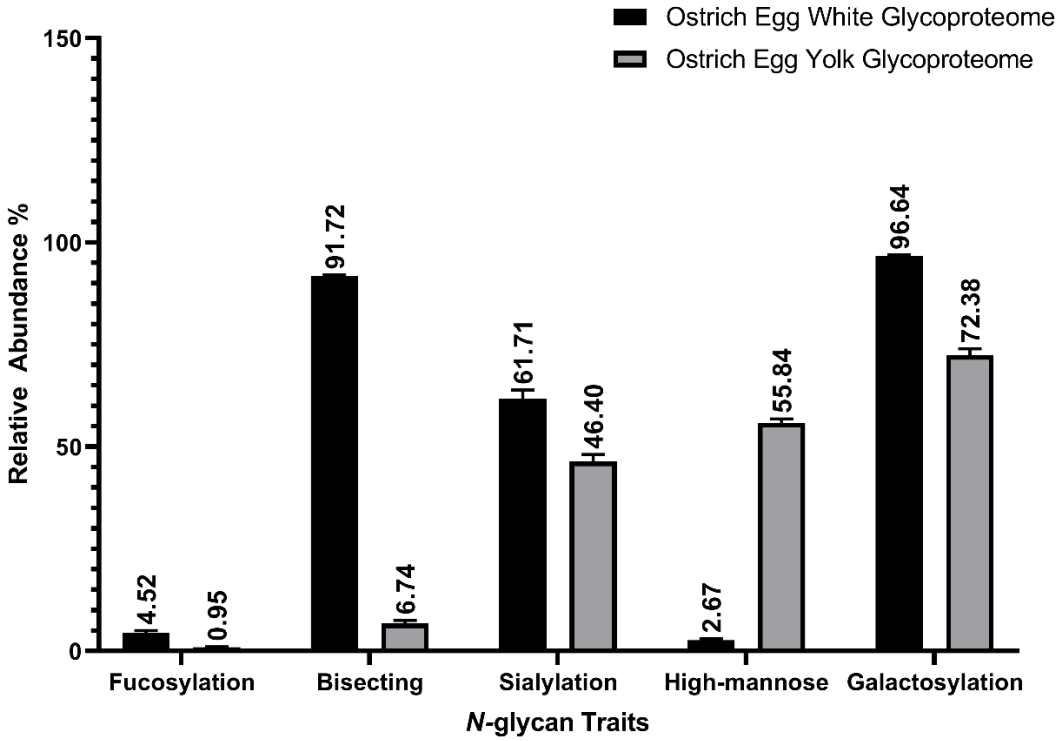

Figure 5: Relative abundances of *N*-glycan traits belonging to ostrich egg white and yolk glycoproteome

Multiple t-test comparisons were also achieved to determine significant changes between both glycoproteomes. The results obtained from multiple t-test analyses were displayed in Table 3. As shown in Table 3 that all *N*-glycan traits obtained from ostrich egg white and yolk glycoproteomes differed significantly at the significant level of $p < 0.01$.

Table 3: Multiple t-test comparison results of *N*-glycan traits.

	P-value	Mean of Ostrich Egg White Glycoproteome	Mean of Ostrich Egg Yolk Glycoproteome	Mean Difference	Standard Error of Difference	t ratio	Fold Ratio
Fucosylation	0.0005	4.52	0.95	3.57	0.35	10.17	4.75
Bisecting	<0.0001	91.72	6.74	84.99	0.59	144.20	13.62
Sialylation	0.0015	61.70	46.40	15.30	1.96	7.80	1.33
High-mannose	<0.0001	2.66	55.84	-53.18	0.71	75.34	0.05
Galactosylation	<0.0001	96.64	72.38	24.26	1.16	21.00	1.34

4. Conclusion

In-depth *N*-glycan profiling of ostrich egg white and yolk glycoproteomes was achieved using a facile glycomics protocol. The number of detected *N*-glycans belonging to ostrich egg white and yolk glycoproteomes was found to be 39 and 36, respectively. Ostrich egg white glycoproteome was highly galactosylated compared to egg yolk. In addition, the abundance of bisecting *N*-glycans was dramatically high in ostrich egg white glycoproteome. However, high-mannose type *N*-glycans were abundant in ostrich egg yolk glycoproteome. This study will contribute to the nutritional glycomics field regarding the structural *N*-glycan analysis of ostrich egg white and yolk glycoproteomes.

Acknowledgments

The author thanks Dr. Bekir Salih for his valued help to use his laboratory facilities and Dr. Sercan Karav for providing ostrich eggs.

References

[1] Başaran, E., Aras, S., Cansaran-Duman, D., *Genomik, proteomik, metabolomik kavramlarına genel bakış ve uygulama alanları*, Türk Hijyen ve Deneysel Biyoloji Dergisi, 67, 85-96, 2010.

[2] Vu, L.D., Gevaert, K., De Smet, I., *Protein language: post-translational modifications talking to each other*, Trends in Plant Science, 23, 1068-1080, 2018.

[3] Oliveira-Ferrer, L., Legler, K., Milde-Langosch, K., *Role of protein glycosylation in cancer metastasis,* Seminars in Cancer Biology, 44, 141-152, 2017.

[4] Mathew, M.P., Donaldson, J.G., *Glycosylation and glycan interactions can serve as extracellular machinery facilitating clathrin- independent endocytosis*, Traffic, 20, 295-300, 2019.

[5] Özaydin, E., Yalçin, F., Gündüz, M., Köse, G., *Konjenital glikozilasyon bozukluğu tip II*, Türkiye Çocuk Hastalıkları Dergisi, 6, 47-53, 2012.

[6] Omana, D.A., Wang, J., Wu, J., *Ovomucin - a glycoprotein with promising potential*. Trends Food Sci Technol., 21, 455-463, 2010.

[7] Kobayashi, K., Hattori, M., Hara-Kudo, Y., Okubo, T., Yamamoto, S., Takita, T., Sugita-Konishi, Y., *Glycopeptide derived from hen egg ovomucin has the ability to bind enterohemorrhagic Escherichia coli O157:H7*, J Agric Food Chemistry, 52, 5740-5746, 2004.

[8] Sharif, M.K., Saleem, M., Javed, K., *Chapter 15 - Food materials science in egg powder industry,* Role of Materials Science in Food Bioengineering, Elsevier press, 505-537, 2018.

[9] Kovacs-Nolan, J., Phillips, M., Mine, Y., *Advances in the value of eggs and egg components for human health,* Journal of Agricultural and Food Chemistry, 53, 8421-8431, 2005.

[10] Smith, D.F., Cummings, R.D., Song, X., *History and future of shotgun glycomics,* Biochemical Society Transactions, 1, 1-11, 2019.

[11] Dong, X., Huang, Y., Cho, B.G., et al., *Advances in mass spectrometry- based glycomics*, Electrophoresıs, 39, 3063-3081, 2018.

[12] Keser, T., Pavić, T., Lauc, G., Gornik, O., *Comparison of 2-Aminobenzamide, Procainamide and RapiFluor-MS as derivatizing agents for High-Throughput HILIC-UPLC-FLR-MS N-Glycan analysis*, Frontiers in Chemistry, 6, 324, 2018.

[13] Kayili, H.M., Avci, İ., Salih, B., *A new Titania Glyco-Purification Tip for the fast enrichment and efficient analysis of glycopeptides and glycans by MALDI-TOF-MS*, Journal of Pharmaceutical and Biomedical Analysis, 174, 191–197, 2019.

[14] Kayili, H.M., Barlas, N., Atakay, M., Salih, B., *Fast purification of glycans and glycopeptides using silk-packed micropipette tip for matrix-assisted laser desorption/ionization-mass spectrometry and high-performance liquid chromatography-fluorescence detection analysis,* Microchemical Journal, 139, 492–499, 2018.

[15] Kayili, H.M., Ertürk, A.S., Elmacı, G., Salih, B., *Poly(Amidoamine) dendrimer-coated magnetic nanoparticles for the fast purification and selective enrichment of glycopeptides and glycans,* Journal of Separation Science, 42, 3209-3216, 2019.

[16] Kozak, R.P., Tortosa, C.B., Fernandes, D.L., Spencer, D.I.R., *Comparison of procainamide and 2-aminobenzamide labeling for profiling and identification of glycans by liquid chromatography with fluorescence detection coupled to electrospray ionization–mass spectrometry*, Analytical Biochemistry, 486, 38-40, 2015.

[17] Kayili, H.M., *Identification of bisecting N-glycans in tandem mass spectra using a procainamide labeling approach for in-depth N-glycan profiling of biological samples*, International Journal of Mass Spectrometry, 457, 116412, 2020.

[18] Nwosu, C., Yau, H.K., Becht, S., *Assignment of core versus Antenna Fucosylation types in protein N-Glycosylation via procainamide labeling and tandem mass spectrometry*, Analytical Chemistry, 87, 5905-5913, 2015.